Nonlinear Analysis of Rayleigh–Taylor Instability of Cylindrical Flow With Heat and Mass Transfer

Mukesh Kumar Awasthi[1]
Department of Mathematics,
Indian Institute of Technology Roorkee,
Roorkee, Uttarakhand 247667, India
e-mail: mukeshiitr.kumar@gmail.com

We study the nonlinear Rayleigh–Taylor instability of the interface between two viscous fluids, when the phases are enclosed between two horizontal cylindrical surfaces coaxial with the interface, and when there is mass and heat transfer across the interface. The fluids are considered to be viscous and incompressible with different kinematic viscosities. The method of multiple expansions has been used for the investigation. In the nonlinear theory, it is shown that the evolution of the amplitude is governed by a Ginzburg–Landau equation. The various stability criteria are discussed both analytically and numerically and stability diagrams are obtained. It has been observed that the heat and mass transfer has stabilizing effect on the stability of the system in the nonlinear analysis. [DOI: 10.1115/1.4024001]

Keywords: Rayleigh–Taylor instability, cylindrical interface, heat and mass transfer, viscous potential flow, nonlinear analysis

1 Introduction

The study of heat and mass transfer across the interface is very important in many situations such as boiling heat transfer in chemical engineering and in geophysical problems. The general formulation of the interfacial flow problem of two inviscid incompressible fluids with heat and mass transfer for Rayleigh–Taylor and Kelvin–Helmholtz instabilities in plane geometry was established by Hsieh [1,2]. Ho [3] studied the linear analysis of Rayleigh–Taylor instability of two viscous fluids of the same kinematic viscosities with heat and mass transfer and observed that heat transfer has a stabilizing effect on the stability of the system. Khodaparast et al. [4] studied the Rayleigh–Taylor and Kelvin–Helmholtz stability of a liquid–vapor interface and considered liquid as viscous and motionless and vapor as inviscid, moving with a horizontal velocity. They observed that coupled viscosity-phase change has a stabilizing effect on Rayleigh– Taylor stability whereas it has a destabilizing effect on Kelvin– Helmholtz instability.

Cylindrical geometry is very important while studying stability problems related to liquid jets and cooling of fuel rods by liquid coolants in the nuclear reactor. Nayak and Chakraborty [5] considered Kelvin–Helmholtz instability of the horizontal cylindrical interface with heat and mass transfer and observed that the plane geometry configuration is more stable than the cylindrical one. The Kelvin–Helmholtz instability of a cylindrical flow with a shear layer has been considered by Wu and Wang [6]. Elhefnawy and Radwan [7] studied the Kelvin–Helmholtz instability of a horizontal cylindrical flow in magnetic fluids in the presence of mass and heat transfer and concluded that the axial magnetic field has a stabilizing effect on the interface, while the effect of a radial magnetic field depends on the choice of some physical parameters present in the system.

In the linear theory, second and higher order terms of perturbed quantities are neglected. Thus, it is clear that such a uniform model based on the linear theory is inadequate to explain the mechanism involved, and hence, the nonlinear theory is needed to reveal the effect of heat and mass transfer on the stability of the system. Hsieh [8] studied the nonlinear Rayleigh–Taylor instability of inviscid fluids in plane geometry taking heat and mass transfer into the account and concluded that nonlinearity increases the stability range when there is heat and mass transfer across the interface. Lee [9] investigated the effect of heat and mass transfer on the Rayleigh–Taylor instability of inviscid fluids in a cylindrical geometry. He observed that in the linear inviscid analysis, heat and mass transfer has no effect on stability criterion; however, it plays an important role in the nonlinear analysis. In the above studies, the stability of two inviscid fluids with heat and mass transfer was discussed.

In viscous potential flow, we consider irrotational flow, so the viscous term, i.e., $\mu\nabla^2\boldsymbol{u}$ in the Navier–Stokes equation is identically zero when the vorticity is zero but the viscous stresses are not zero, where μ denotes the viscosity and $\boldsymbol{u}$ denotes the velocity of the fluid flow. There exists a pressure difference across the interface. We include normal stress for calculating this pressure difference and the viscosity enters through the normal stress balance (Joseph and Liao [10]). Tangential stresses are not considered in the viscous potential flow theory. As such, we cannot enforce a no-slip condition on the boundary. Joseph et al. [11] applied viscous potential flow analysis to study the Rayleigh–Taylor instability in plane geometry and found that the most dangerous wave is one whose length gives the maximum growth rate. Joseph et al. [12] extended the study of Rayleigh–Taylor instability to the viscoelastic fluids at high Weber numbers and concluded that the most unstable wave is sensitive function of the retardation time. Asthana et al. [13] studied the viscous potential flow analysis of Rayleigh–Taylor instability in the cylindrical geometry and observed that viscous normal stresses stabilize the system.

Viscous potential flow analysis of Kelvin–Helmholtz instability with heat and mass transfer in plane geometry was carried out by Asthana and Agrawal [14]. They observed that heat and mass transfer has a strong stabilizing effect when the lower fluid is highly viscous, and a weak destabilizing effect when the fluid's viscosity is low. Awasthi and Agrawal [15] studied the effect of heat and mass transfer on the Rayleigh–Taylor instability in plane geometry when there is heat and mass transfer across the interface and observed that heat and mass transfer has a stabilizing effect. Viscous potential flow analysis of capillary instability with heat and mass transfer has been considered by Kim et al. [16]. They

[1]Present address: Department of Mathematics, Graphic Era University, Dehradun 248002, India.

Contributed by the Fluids Engineering Division of ASME for publication in the JOURNAL OF FLUIDS ENGINEERING. Manuscript received October 3, 2012; final manuscript received March 4, 2013; published online April 12, 2013. Assoc. Editor: Ye Zhou.

observed that heat and mass transfer is stabilizing the interface against capillary effects for the irrotational motion of two viscous fluids. Awasthi and Agrawal [17] studied the nonlinear capillary instability using viscous potential flow theory when there is heat and mass transfer across the interface, finding that the heat and mass transfer is stabilizing the interface.

In view of the above investigations and keeping in mind the importance of heat and mass transfer in various applications such as boilers, condensers, reactors, and other industrial processes, a study of the nonlinear Rayleigh–Taylor instability of cylindrical interface when there is heat and mass transfer across the interface is attempted. Both fluids are taken as incompressible and viscous with different kinematic viscosities, which were not considered earlier. We used the method of multiple expansions for the investigation and the evolution of amplitude is shown to be governed by a nonlinear Ginzburg–Landau equation. Stability is discussed theoretically as well as numerically, and the stability region has been displayed graphically. In addition, a comparative analysis has been made between the results obtained in the inviscid flow analysis (Ref. [9]) and present viscous flow analysis. The paper is structured as follows: in Sec. 2 mathematical formulation of the problem has been given. The first order theory and linear dispersion relation was obtained in Sec. 3. In Sec. 4, the second order solution is derived. A Ginzburg–Landau equation is obtained in Sec. 5. In Sec. 6, we compared our results with available results in the literature. The numerical discussion along with the graphic forms is given in Sec. 7. Finally, a summary of our findings is given in Sec. 8.

2 Problem Formulation

A system of two incompressible and viscous fluids, separated by a cylindrical interface, is considered in an annular configuration as shown in Fig. 1. A cylindrical system of coordinates (r, θ, z) is assumed so that in the equilibrium state, the z-axis is the axis of symmetry of the system. The undisturbed cylindrical interface is taken at radius R. In the formulation, the superscripts 1 and 2 denote the variables associated with the fluid inside and outside the interface, respectively. Both fluid phases are assumed to be incompressible and irrotational. In the undisturbed state, viscous fluid of thickness h_1, density $\rho^{(1)}$ and viscosity $\mu^{(1)}$ occupies the inner region $r_1 < r < R$ and viscous fluid of thickness h_2, density $\rho^{(2)}$, and viscosity $\mu^{(2)}$ occupies the outer region $R < r < r_2$. Surface tension at the interface is taken as σ. The bounding surfaces $r = r_1$ and $r = r_2$ are considered to be rigid. The temperatures at $r = r_1, r = R,$ and $r = r_2$ are $T_1, T_0,$ and T_2, respectively.

On applying the small axisymmetric disturbances to the equilibrium state, the interface can be expressed as:

$$F(r, z, t) = r - R - \eta(z, t) = 0 \quad (2.1)$$

where η is the perturbation in the radius of the interface from the equilibrium value R, and for which the outward unit normal vector is given by

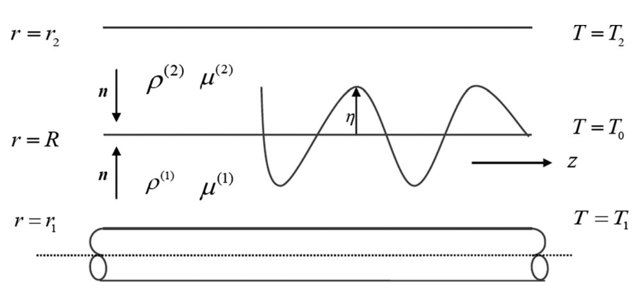

Fig. 1 Equilibrium configuration of the system

$$\boldsymbol{n} = \frac{\nabla F}{|\nabla F|} = \left\{1 + \left(\frac{\partial \eta}{\partial z}\right)^2\right\}^{-1/2} \left(\boldsymbol{e_r} - \frac{\partial \eta}{\partial z}\boldsymbol{e_z}\right) \quad (2.2)$$

where $\boldsymbol{e_r}$ and $\boldsymbol{e_z}$ are unit vectors along the r and z directions, respectively.

The velocity is expressed as the gradient of a potential function and the potential functions satisfy the Laplace equation as a consequence of the incompressibility constraint. That is,

$$\nabla^2 \phi^{(j)} = 0 \quad (j = 1, 2) \quad (2.3)$$

At the walls normal velocity vanishes; hence,

$$\frac{\partial \phi^{(j)}}{\partial r} = 0 \quad \text{at} \quad r = r_j \quad \text{for} \quad (j = 1, 2) \quad (2.4)$$

It is assumed that phase-change takes place locally in such a way that the net phase-change rate at the interface is equal to zero. Lee [9] derived the interfacial mass and heat transfer conditions for Rayleigh–Taylor instability of cylindrical flow. The interfacial condition, which expresses the conservation of mass across the interface, is given by the equation

$$\left[\!\left[\rho\left(\frac{\partial F}{\partial t} + \nabla\phi \cdot \nabla F\right)\right]\!\right] = 0 \quad (2.5)$$

where $[\![\cdot]\!]$ represents the difference in a quantity across the interface. Using Eqs. (2.1) and (2.5) we get

$$\left[\!\left[\rho\left(\frac{\partial \phi}{\partial r} - \frac{\partial \eta}{\partial t} - \frac{\partial \eta}{\partial z}\frac{\partial \phi}{\partial z}\right)\right]\!\right] = 0 \quad \text{at} \quad r = R + \eta \quad (2.6)$$

The interfacial condition for energy transfer proposed by Lee [9] is expressed as

$$L\rho^{(1)}\left(\frac{\partial F}{\partial t} + \nabla\phi^{(1)} \cdot \nabla F\right) = S(\eta) \quad \text{at} \quad r = R + \eta \quad (2.7)$$

where L is the latent heat released during phase transformation and $S(\eta)$ denotes the net heat flux from the interface. In deriving Eq. (7), Lee [9] assumed that the amount of latent heat released depends mainly on the instantaneous position of the interface.

In the equilibrium state, the heat fluxes in the positive r-direction in the fluid phases 1 and 2, which are $-K_1(T_1 - T_0)/R\ln(R_1/R)$ and $-K_2(T_0 - T_2)/R\ln(R/R_2)$, respectively, where K_1 and K_2 denote the heat conductivities of the two fluids. The expression for $S(\eta)$ as proposed by Nayak and Chakraborty [5] for the cylindrical geometry is

$$S(\eta) = \frac{K_2(T_0 - T_2)}{(R+\eta)(\ln r_2 - \ln(R+\eta))} - \frac{K_1(T_1 - T_0)}{(R+\eta)(\ln(R+\eta) - \ln r_1)} \quad (2.8)$$

On expanding $S(\eta)$ about $r = R$, i.e., at $\eta = 0$,

$$S(\eta) = S(0) + \eta S'(0) + \frac{1}{2}\eta^2 S''(0) + \frac{1}{6}\eta^3 S'''(0) + \cdots \quad (2.9)$$

Since $S(0) = 0$, from Eq. (2.8) we get:

$$\frac{K_2(T_0 - T_2)}{R\ln(r_2/R)} = \frac{K_1(T_1 - T_0)}{R\ln(R/r_1)} = G, \text{where } G \text{ is a constant} \quad (2.10)$$

hence in the equilibrium state, heat fluxes across the interfaces are equal.

Using Eq. (2.1), with the Eqs. (2.7)–(2.10), the equation of energy transfer becomes:

$$\rho^{(1)}\left(\frac{\partial\phi^{(1)}}{\partial r}-\frac{\partial\eta}{\partial t}-\frac{\partial\eta}{\partial z}\frac{\partial\phi^{(1)}}{\partial z}\right)=\alpha\left(\eta+\alpha_2\eta^2+\alpha_3\eta^3\right) \tag{2.11}$$

where $\alpha=\dfrac{G\log(r_2/r_1)}{LR\log(r_2/R)\log(R/r_1)}$,

$$\alpha_2=\frac{1}{R}\left(-\frac{3}{2}+\frac{1}{\log(r_2/R)}-\frac{1}{\log(R/r_1)}\right)$$

$$\alpha_3=\frac{1}{R^2}\left(\frac{11}{6}-\frac{2\log(R^2/r_1r_2)}{\log(r_2/R)\log(R/r_1)}+\frac{\log^3(r_2/R)+\log^3(R/r_1)}{[\log(r_2/R)\log(R/r_1)]^2\log(r_2/r_1)}\right)$$

With mass transfer across the interface, interfacial condition for the conservation of momentum is given by

$$\begin{aligned}&\rho^{(1)}(\nabla\phi^{(1)}\cdot\nabla F)\left(\frac{\partial F}{\partial t}+\nabla\phi^{(1)}\cdot\nabla F\right)\\&=\rho^{(2)}(\nabla\phi^{(2)}\cdot\nabla F)\left(\frac{\partial F}{\partial t}+\nabla\phi^{(2)}\cdot\nabla F\right)\\&+(p_2-p_1-2\mu^{(2)}\boldsymbol{n}\cdot\nabla\otimes\nabla\phi^{(2)}\cdot\boldsymbol{n}\\&+2\mu^{(1)}\boldsymbol{n}\cdot\nabla\otimes\nabla\phi^{(1)}\cdot\boldsymbol{n}+\sigma\nabla\cdot\boldsymbol{n})|\nabla F|^2\end{aligned} \tag{2.12}$$

where p represents the pressure, σ denotes the surface tension coefficient, and $\boldsymbol{n}$ is the unit normal vector at the interface. Surface tension has been assumed to be a constant, neglecting its dependence on temperature.

Eliminating the pressure term using Bernoulli's equation, Eq. (2.12) reduces to

$$\begin{aligned}&\left[\!\!\left[\rho\left\{\frac{\partial\phi}{\partial t}+\frac{1}{2}\left[\left(\frac{\partial\phi}{\partial r}\right)^2+\left(\frac{\partial\phi}{\partial z}\right)^2\right]-\left\{1+\left(\frac{\partial\eta}{\partial z}\right)^2\right\}^{-1}\right.\right.\right.\\&\left.\times\left(\frac{\partial\phi}{\partial r}-\frac{\partial\eta}{\partial z}\frac{\partial\phi}{\partial z}\right)\left(\frac{\partial\phi}{\partial r}-\frac{\partial\eta}{\partial t}-\frac{\partial\eta}{\partial z}\frac{\partial\phi}{\partial z}\right)\right\}\\&\left.\left.+2\mu\left\{1+\left(\frac{\partial\eta}{\partial z}\right)^2\right\}^{-1}\left[\frac{\partial^2\phi}{\partial r^2}-2\frac{\partial\eta}{\partial z}\frac{\partial^2\phi}{\partial r\partial z}+\left(\frac{\partial\eta}{\partial z}\right)^2\frac{\partial^2\phi}{\partial z^2}\right]\right]\!\!\right]\\&=-\sigma\left[\left(\frac{\partial^2\eta}{\partial z^2}\right)\left\{1+\left(\frac{\partial\eta}{\partial z}\right)^2\right\}^{-3/2}+\sigma(R+\eta)^{-1}\right.\\&\left.\times\left\{1+\left(\frac{\partial\eta}{\partial z}\right)^2\right\}^{-1/2}\right]\end{aligned} \tag{2.13}$$

We are using spatiotemporal multiple expansion method (Ref. [9]) to study the nonlinear stability analysis of the considered system. Let us assume the following expansion of the variables:

$$\eta=\sum_{n=1}^{3}\varepsilon^n\eta_n(z_0,z_1,z_2,t_0,t_1,t_2)+O(\varepsilon^4) \tag{2.14}$$

$$\phi^{(j)}=\sum_{n=1}^{3}\varepsilon^n\phi_n^{(j)}(r,z_0,z_1,z_2,t_0,t_1,t_2)+O(\varepsilon^4) \tag{2.15}$$

where ε is a small parameter indicating the order of the perturbation and $z_n=\varepsilon^n z, t_n=\varepsilon^n t(n=0,1,2)$. The variables η and $\phi^{(j)}$ appearing in Eqs. (2.6), (2.11), and (2.13) are expressed in Maclaurin series around $r=R$. Then we used the expression for η and $\phi^{(j)}$ from Eqs. (2.14) and (2.15) in the equation so obtained. Finally, we equate the coefficients of equal powers in ε to obtain the linear and the successive nonlinear partial differential equations of various orders.

3 Linear Theory

The solution of Eq. (2.3) using the boundary conditions, can be written as

$$\eta_1=A(z_1,z_2,t_1,t_2)e^{i\vartheta}+\bar{A}(z_1,z_2,t_1,t_2)e^{-i\vartheta} \tag{3.1}$$

$$\phi_1^{(1)}=\frac{1}{k}\left(\frac{\alpha}{\rho^{(1)}}-i\omega\right)A(z_1,z_2,t_1,t_2)E^{(1)}(kr)e^{i\vartheta}+c.c. \tag{3.2}$$

$$\phi_1^{(2)}=\frac{1}{k}\left(\frac{\alpha}{\rho^{(2)}}-i\omega\right)A(z_1,z_2,t_1,t_2)E^{(2)}(kr)e^{i\vartheta}+c.c. \tag{3.3}$$

where

$$E^{(1)}(kr)=\frac{I_0(kr)K_1(kr_1)+I_1(kr_1)K_0(kr)}{I_1(kR)K_1(kr_1)-I_1(kr_1)K_1(kR)} \tag{3.4}$$

$$E^{(2)}(kr)=\frac{I_0(kr)K_1(kr_2)+I_1(kr_2)K_0(kr)}{I_1(kR)K_1(kr_2)-I_1(kr_2)K_1(kR)} \tag{3.5}$$

$$\vartheta=kz_0-\omega t_0$$

with $I_m(kr)$ and $K_m(kr)(m=0,1)$ representing the modified Bessel functions of the first and second kinds of order m, respectively.

Substituting Eqs. (3.1)–(3.3) into the linear form of the momentum equation, we get

$$D(\omega,k)=a_0\omega^2+ia_1\omega+a_2=0 \tag{3.6}$$

where $a_0=\rho^{(1)}E^{(1)}(kR)-\rho^{(2)}E^{(2)}(kR)$

$$a_1=\alpha(E^{(1)}(kR)-E^{(2)}(kR))+2k^2(\mu_1F^{(1)}(kR)-\mu_2F^{(2)}(kR))$$

$$a_2=-\sigma k(k^2-\frac{1}{R^2})-2k^2\alpha\left(\frac{\mu^{(1)}}{\rho^{(1)}}F^{(1)}(kR)-\frac{\mu^{(2)}}{\rho^{(2)}}F^{(2)}(kR)\right)$$

$$F^{(1)}(kR)=E^{(1)}(kR)-\frac{1}{kR},\quad F^{(2)}(kR)=E^{(2)}(kR)-\frac{1}{kR}$$

when there is no heat and mass transfer ($\alpha=0$) across the interface, Eq. (3.6) reduces to the same expression as obtained by Asthana et al. [13].

On applying Routh–Hurwitz criteria in Eq. (3.6), the stability condition can be written as $a_0>0, a_1>0, a_2>0$.

Using the properties of Modified Bessel functions, we have $a_0>0$ trivially, and since $\alpha,\mu^{(2)}$, and $\mu^{(1)}$ are positive, $a_1>0$.

As such, the condition of stability gives rise to $a_2>0$ and the condition of marginal state is given by $a_2=0$

$$\text{i.e.:}\quad \sigma\left(k_c^2-\frac{1}{R^2}\right)+2k_c\alpha\left(\frac{\mu^{(1)}}{\rho^{(1)}}F^{(1)}(k_cR)-\frac{\mu^{(2)}}{\rho^{(2)}}F^{(2)}(k_cR)\right)=0 \tag{3.7}$$

It can be concluded that if fluids are inviscid ($\mu^{(1)}=\mu^{(2)}=0$), heat transfer has no effect on the stability criteria.

4 Second-Order Solution

Using the first-order solution, the equation for second order solution is given by

$$\nabla_0^2\phi_2^{(j)}=-2i\left(\frac{\alpha}{\rho^{(j)}}-i\omega\right)E^{(j)}(kr)\frac{\partial A}{\partial z_1}\quad (j=1,2) \tag{4.1}$$

where

$$\nabla_0^2=\frac{\partial^2}{\partial r^2}+\frac{1}{r}\frac{\partial}{\partial r}+\frac{\partial^2}{\partial z_0^2}$$

and the boundary conditions at $r=R$

$$\rho^{(j)}\left\{\frac{\partial\phi_2^{(j)}}{\partial r}-\frac{\partial\eta_2}{\partial t_0}\right\}-\alpha\eta_2$$

$$=\left[\rho^{(j)}\left\{\frac{\alpha}{\rho^{(j)}}-i\omega\right\}\left\{\frac{1}{R}-2kE^{(j)}(kR)\right\}+\alpha\alpha_2\right]A^2e^{2i\vartheta}$$

$$+\rho^{(j)}\frac{\partial A}{\partial t_1}e^{i\vartheta}+c.c.+2\alpha\left(\frac{1}{R}+\alpha_2\right)|A|^2\quad(j=1,2)\tag{4.2}$$

$$\rho^{(2)}\frac{\partial\phi_2^{(2)}}{\partial r}-\rho^{(1)}\frac{\partial\phi_2^{(1)}}{\partial r}-\left\{\rho^{(2)}-\rho^{(1)}\right\}\frac{\partial\eta_2}{\partial t_0}$$

$$=\left[\!\left[\rho\left(\frac{\alpha}{\rho}-i\omega\right)\left(\frac{1}{R}-2kE(kR)\right)\right]\!\right]A^2e^{2i\vartheta}$$

$$+\left\{\rho^{(2)}-\rho^{(1)}\right\}\frac{\partial A}{\partial t_1}e^{i\vartheta}+c.c.\tag{4.3}$$

$$\left[\!\left[\rho\frac{\partial\phi_2}{\partial t_0}+2\mu\frac{\partial^2\phi_2}{\partial r^2}\right]\!\right]+\sigma\left(\frac{\partial^2\eta_2}{\partial z^2}+\frac{\eta_2}{R^2}\right)$$

$$=\left\{-\frac{\omega^2}{2}[\![\rho\{E^2(kR)-3\}]\!]+\frac{\alpha^2}{2\rho}[\![1+E^2(kR)]\!]\right.$$

$$-i\alpha\omega[\![E^2(kR)]\!]-2\mu k^2\left[\!\left[\left(\frac{\alpha}{\rho}-i\omega\right)\left(3+\frac{2}{k^2R^2}-\frac{E(kR)}{kR}\right)\right]\!\right]$$

$$\left.+\frac{\sigma}{2R^3}(R^2k^2+2)\right\}A^2e^{2i\vartheta}-\left[\!\left[\frac{\rho}{k}\left(\frac{\alpha}{\rho}-i\omega\right)E(kR)\right]\!\right]\frac{\partial A}{\partial t_1}e^{i\vartheta}$$

$$+c.c.+\left[\left[\!\left[\rho\left(\frac{\alpha^2}{\rho^2}+\omega^2\right)\{1-E^2(kR)\}\right.\right.\right.$$

$$\left.\left.+\frac{4\mu\alpha k^2}{\rho}\left(1+\frac{2}{k^2R^2}+\frac{E(kR)}{kR}\right)\right]\!\right]-\frac{\sigma}{R^3}(R^2k^2-2)\right]|A|^2\tag{4.4}$$

The nonsecularity conditions for the existence of the uniformly valid solutions are

$$\frac{\partial A}{\partial t_1}+V_g\frac{\partial A}{\partial z_1}=0\tag{4.5}$$

and its conjugate relation. Here, V_g denotes the group velocity of the wave and defined as

$$V_g=\frac{d\omega}{dk}$$

The solution of Eqs. (4.1)–(4.4) gives rise to

$$\eta_2=-2\left(\frac{1}{R}+\alpha_2\right)|A|^2+A_2e^{2i\vartheta}+\bar{A}_2e^{-2i\vartheta}\tag{4.6}$$

$$\phi_2^{(j)}=\left[-\frac{i}{k}\left\{\frac{\alpha}{\rho^{(j)}}-i\omega\right\}\left\{rL_1^{(j)}(kr)+r_jL_2^{(j)}(kr)\right.\right.$$

$$\left.\left.-\left[RE^{(j)}(kR)-r_jL_3^{(j)}(kR)\right]E^{(j)}(kr)\right\}\frac{\partial A}{\partial z_1}+\frac{1}{k}\frac{\partial A}{\partial t_1}E^{(j)}(kr)\right]e^{i\vartheta}$$

$$+B_2^{(j)}E^{(j)}(2kr)A^2e^{2i\vartheta}+c.c.+b^{(j)}(t_0,t_1,t_2)\quad(j=1,2)\tag{4.7}$$

where

$$A_2=-\frac{2k}{D(2\omega,2k)}\left\{\left[\!\left[\rho\frac{i\omega}{k}E(2kR)\beta+\frac{\rho}{2}E^2(kR)\left(\frac{\alpha}{\rho}-i\omega\right)^2\right.\right.\right.$$

$$+\frac{3\omega^2\rho^2+\alpha^2}{2\rho}-4\mu k\beta F(2kR)-2k^2\mu\left(\frac{\alpha}{\rho}-i\omega\right)$$

$$\left.\left.\times\left(3+\frac{2}{k^2R^2}-\frac{E(kR)}{kR}\right)\right]\!\right]+\frac{\sigma}{2R^3}(k^2R^2+2)\right\}|A|^2\tag{4.8}$$

$$B_2^{(j)}=\frac{1}{2k}\left[\beta^{(j)}A^2+\left(\frac{\alpha}{\rho^{(j)}}-2i\omega\right)A_2\right]\tag{4.9}$$

$$\beta^{(j)}=\left(\frac{\alpha}{\rho^{(j)}}-i\omega\right)\left(\frac{1}{R}-2kE^{(j)}(kR)\right)+\frac{\alpha\alpha_2}{\rho^{(j)}}\tag{4.10}$$

$$\rho^{(2)}\frac{\partial b^{(2)}}{\partial t}-\rho^{(1)}\frac{\partial b^{(1)}}{\partial t}=\left\{\left[\!\left[\rho\left(\frac{\alpha^2}{\rho^2}+\omega^2\right)\{1-E_n^2(kR)\}+\frac{4\mu\alpha k^2}{\rho}\right.\right.\right.$$

$$\left.\times\left(1+\frac{2}{k^2R^2}+\frac{E(kR)}{kR}\right)\right]\!\right]$$

$$\left.-\frac{\sigma}{R^3}(R^2k^2-4-2R\alpha_2)\right\}|A|^2\tag{4.11}$$

$$L_1^{(j)}(kr)=\frac{I_1(kr)K_1(kr_j)-I_1(kr_j)K_1(kr)}{I_1(kR)K_1(kr_j)-I_1(kr_j)K_1(kR)},$$

$$L_2^{(j)}=\frac{K_0(kr)I_0(kr_j)-K_0(kr_j)I_0(kr)}{I_1(kR)K_1(kr_j)-I_1(kr_j)K_1(kR)},$$

$$L_3^{(j)}(kr)=\frac{I_0(kr_j)K_1(kR)+I_1(kR)K_0(kr_j)}{I_1(kR)K_1(kr_j)-I_1(kr_j)K_1(kR)}$$

Here, we assumed that $D(2\omega,2k)\neq 0$.

5 Third-Order Solution

For the third-order solution, we have

$$\nabla_0^2\phi_3^{(j)}=-\frac{\partial^2\phi_1^{(j)}}{\partial z_1^2}-2\frac{\partial^2\phi_1^{(j)}}{\partial z_0\partial z_2}-2\frac{\partial^2\phi_2^{(j)}}{\partial z_0\partial z_1}\quad(j=1,2)\tag{5.1}$$

On substituting the values of η_1 and $\phi_1^{(j)}$ from Eqs. (3.1)–(3.3) and η_2 and $\phi_2^{(j)}$ from Eqs. (4.6)–(4.7), the expressions for $\phi_3^{(j)}$ can be written as

$$\phi_3^{(j)}=-\frac{1}{k}\left\{\frac{\alpha}{\rho^{(j)}}-i\omega\right\}\left[\frac{1}{2}\left\{r^2E^{(j)}(kr)-\frac{r}{k}L_1^{(j)}(kr)\right\}-rr_jL_3^{(j)}(kr)\right.$$

$$-\left\{rE^{(j)}(kr)-r_jL_3^{(j)}(kr)\right\}rL_1^{(j)}(kr)+\frac{1}{k}M^{(j)}(kr)$$

$$\times\left\{\frac{r_j}{k}E^{(j)}(kr_j)-\left\{RE^{(j)}(kr)-r_jL_3^{(j)}(kr)\right\}kr_jE^{(j)}(kr_j)\right\}$$

$$-\left\{\frac{R}{2}\left(E^{(j)}(kr)+2k\right)+Rk\left\{r_jL_2^{(j)}(kr)-\left\{RE^{(j)}(kr)\right.\right.\right.$$

$$\left.\left.\left.\left.-r_jL_3^{(j)}(kr)\right\}E^{(j)}(kr)\right\}\frac{E^{(j)}(kr_j)}{k}\right\}\right]\frac{\partial^2A}{\partial z_1^2}e^{i\theta}-\frac{i}{k}\left\{rL_1^{(j)}(kr)\right.$$

$$\left.+r_jL_2^{(j)}(kr)-(RE^{(j)}(kR)-r_jL_3^{(j)}(kR))E^{(j)}(kr)\right\}$$

$$\times\left[\left\{\frac{\alpha}{\rho^{(j)}}-i\omega\right\}\frac{\partial A}{\partial z_2}+\frac{\partial^2A}{\partial z_1\partial t_1}\right]e^{i\theta}+\frac{E^{(j)}(kr)}{k}\frac{\partial A}{\partial t_2}e^{i\theta}$$

$$+C_3^{(j)}\quad(j=1,2)\tag{5.2}$$

here

$$C_3^{(j)}=-kE^{(j)}(kr)\left[2\left\{E^{(j)}(2kR)-\frac{1}{kR}\right\}B_2^{(j)}\right.$$

$$+\left\{-2\left\{E^{(j)}(kR)-\frac{1}{kR}\right\}\left(\frac{\alpha}{\rho^{(j)}}-i\omega\right)\left(\frac{1}{kR}+\frac{\alpha_2}{k}\right)\right.$$

$$+\frac{1}{2}\left(1+\frac{2}{k^2R^2}-\frac{E^{(j)}(kR)}{Rk}\right)\left(\frac{3\alpha}{\rho^{(j)}}-i\omega\right)-\frac{\alpha}{\rho^{(j)}}-i\omega$$

$$\left.+\frac{\alpha}{\rho^{(j)}k^2}\left\{4\alpha_2\left(\frac{1}{R}+\alpha_2\right)-3\alpha_3\right\}\right\}A^2$$

$$\left.-\left\{\left(\frac{\alpha}{\rho^{(j)}}+i\omega\right)\left(E^{(j)}(kR)+\frac{1}{kR}\right)+\frac{2\alpha\alpha_2}{\rho^{(j)}k}\right\}\frac{A_2}{k}\right]\bar{A}e^{i\theta}$$

$$+H_1E^{(j)}(2kr)e^{2i\theta}+J_1E^{(j)}(3kr)e^{3i\theta}+c.c.$$

where the expressions for H_1 and J_1 can be determined from the boundary conditions.

The third order solution, along with the condition for third order perturbation to be nonsecular, can be written as

$$i\left(\frac{\partial A}{\partial t_2}+V_g\frac{\partial A}{\partial z_2}\right)+P\frac{\partial^2 A}{\partial z_1^2}=QA^2\bar{A}+RA \tag{5.3}$$

here

$$P=\frac{1}{2}\frac{\partial V_g}{\partial k}$$

$$R=-\upsilon\frac{\partial D}{\partial k}\left(\frac{\partial D}{\partial \omega}\right)^{-1}$$

where υ can be defined as $k=k_c+\upsilon\varepsilon^2$ with k_c equals to critical wave number.

Introducing the transformations (Ref. [9])

$$\varsigma=\varepsilon^{-1}(z_2-V_g t_2)=(z_1-V_g t_1)=\varepsilon(z-V_g t) \text{ and } \tau=t_2=\varepsilon t_1 =\varepsilon^2 t$$

Equation (5.3) becomes

$$i\frac{\partial A}{\partial \tau}+P\frac{\partial^2 A}{\partial \varsigma^2}=QA^2\bar{A}+RA \tag{5.4}$$

Equation (5.4) is a complex Ginzburg–Landau equation, i.e., P, Q, and R are complex quantities.

The stability of the Ginzburg–Landau equation (Eq. (5.4)) has been discussed by Lange and Newell [18]. They showed that the stability conditions are

$$P_rQ_r+P_iQ_i>0 \quad \text{and} \quad Q_i<0 \tag{5.5}$$

provided that $R_r=0$.

It was found that the condition $R_r=0$ is satisfied when $\omega=0$, and $P_r=Q_r=0$. Using these conditions, Eq. (5.4) reduces to the nonlinear diffusion equation,

$$\frac{\partial A}{\partial \tau}+P_i\frac{\partial^2 A}{\partial \varsigma^2}=Q_iA^2\bar{A}+R_iA \tag{5.6}$$

where

$$\begin{aligned}Q_i=\frac{k}{a_1}\Bigg[\Bigg[\!\Bigg[&\rho\left\{2kB_2\left(\frac{\alpha}{\rho}\{E(kR)E(2kR)-1\}\right)+\frac{3\alpha^2}{\rho^2}\right\}\\&+2\mu k^2\left\{C_3F(kR)+4kB_2\left(\frac{1}{k^2R^2}-\frac{E(2kR)}{kR}\right)\right.\\&-\frac{2\alpha}{\rho}\left(\frac{1}{R}+\alpha_2\right)\left(1+\frac{2}{k^2R^2}-\frac{E(kR)}{kR}\right)\\&+\frac{\alpha}{\rho}\left(\frac{1}{R}+\frac{2}{k^2R^2}-\frac{E(kR)}{kR}-3\right)A_2\\&\left.-\frac{k\alpha}{\rho}\left(\frac{5E(kR)}{2}+\frac{9E(kR)}{2k^2R^2}+\frac{9}{k^3R^3}\right)\right\}\Bigg]\!\Bigg]\\&+\frac{\sigma}{R^4}\left\{2RA_2\left(k^2R^2-1\right)+4R\alpha_2+7-\frac{1}{2}k^2R^2\left(1-3k^2R^2\right)\right\}\Bigg]\end{aligned}$$

If fluids are inviscid ($\mu^{(1)}=\mu^{(2)}=0$), the expression for Q_i is reduced in the same expression as obtained by Lee [9].

The solution of the nonlinear diffusion equation (Eq. (5.6)) is valid near the marginal state, i.e., $\omega=0$, and therefore is used to study the stability of the system. Near the marginal state, the inequalities (Eq. 5.5)) reduces to

$$P_i<0 \quad \text{and} \quad Q_i<0 \tag{5.7}$$

6 Comparison With Previous Results

Lee [9] studied the nonlinear Rayleigh–Taylor instability of inviscid fluids in a cylindrical geometry when there is heat and mass transfer across the interface. He took the nondimensional parameter $\delta=R^3\alpha/\rho^{(1)}\sigma$ and obtained the values of δ for which the system is stable. We compared our results with the results obtained by Lee [9] to study the effect of viscosity on the considered system in Figs. 2 and 3. We took the following parametric values as considered by Lee [9]:

$$\rho^{(1)}=3.652\times10^{-4}\ \text{gm/cm}^3,\quad \rho^{(2)}=5.97\times10^{-2}\ \text{gm/cm}^3,$$
$$\sigma=0.06\ \text{dyne/cm}\quad \mu^{(1)}=0.00018\ \text{poise},\quad \mu^{(2)}=0.01\ \text{poise},$$

In Fig. 2, we plotted the variation of nondimensional parameter δ with respect to the vapor thickness h_1 for the inviscid potential flow analysis (Ref. [9]) and viscous potential flow analysis when $r_1=1$ cm and $r_2=2$ cm, taking heat and mass transfer into the account. The region above the curve is the stable region, while the region below the curve is the region of instability. It was observed that the marginal stability curve obtained for VPF solution is below in comparison to the IPF solution. Viscous potential flow analysis contains the effect of normal stresses while inviscid potential flow ignores the contribution of viscosity at all. This indicates that VPF solution is more stable than the IPF solution. In other words, we can say, the effect of viscosity is stabilizing the liquid-vapor interface in the nonlinear analysis.

Figure 3 shows a comparison between the neutral curves of nondimensional parameter δ with respect to the vapor thickness h_1 for the inviscid potential flow analysis (Ref. [9]) and viscous potential flow analysis when $r_1=1$ cm and $r_2=5$ cm. It was observed that, in this case, the curves shift upwards; however, the trend is similar as in Fig. 2. It concludes that on increasing the annular region, the disturbance waves grow.

7 Numerical Results and Discussion

In this section, the numerical computation has been carried out using the stability expression (Eq. (5.7)) for a film boiling condition. Steam and water have been taken as working fluids identified with phase 1 and phase 2, respectively, such that $T_1>T_0>T_2$. We treat steam as incompressible since the Mach number is expected to be small. In film boiling, the water-steam interface is in saturation condition and the temperature T_0 is equal to the saturation temperature.

$$\rho^{(1)}=0.001\ \text{gm/cm}^3,\quad \rho^{(2)}=1.0\ \text{gm/cm}^3$$

$$\mu^{(1)}=0.00001\ \text{poise},\quad \mu^{(2)}=0.01\ \text{poise},\quad \sigma=72.3\ \text{dyne/cm}$$

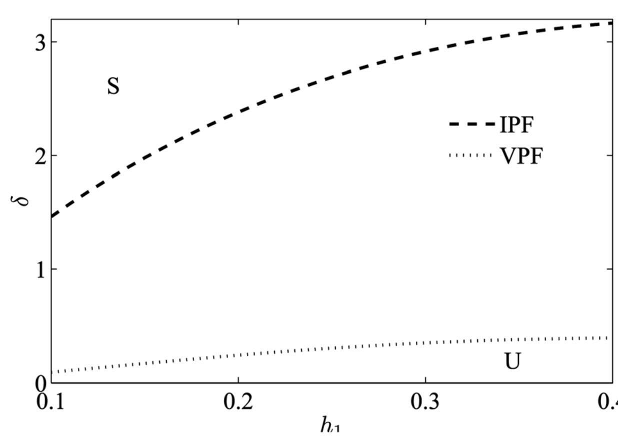

Fig. 2 Comparison between the neutral stability curves obtained for the IPF analysis as well as VPF analysis for r_1 = 1 cm and r_2 = 2 cm

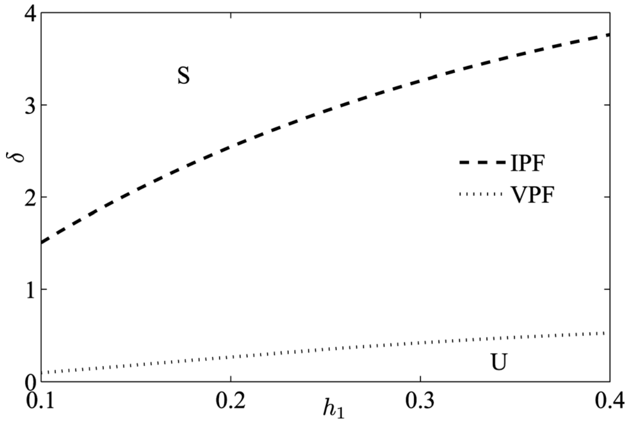

Fig. 3 Comparison between the neutral stability curves obtained for the IPF analysis as well as VPF analysis for r_1 = 1 cm and r_2 = 5 cm

The radii of the inner and outer cylinder are 1 cm and 2 cm, respectively. At the interface, phase change is taking place. The stable and unstable regions are shown in the following figures. 'S' and 'U' denote nonlinearly stable and unstable regions, respectively. In the following paragraphs, the effect of various physical parameters on the onset of instability is interpreted through various figures.

The variation of wave number k with respect to vapor thickness h_1 for the different values of heat transfer coefficient α is shown in Fig. 4. The neutral stability curves divide the plane into the unstable region above the curve and stable region below the curve. It is also observed that, as the heat transfer coefficient increases, the stable region increases, which shows that the heat and mass transfer phenomenon is stabilizing the classically unstable system. The effect of heat and mass transfer can be explained in terms of local evaporation and condensation at the interface. At a perturbed interface, crests are warmer because they are closer to the hotter boundary on the vapor side; thus local evaporation takes place, whereas troughs are cooler and thus condensation will take place. The liquid is protruding to a hotter region and the evaporation will diminish the growth of disturbance waves. It can also be seen from Fig. 4 that, as vapor thickness increases, the stable region decreases. In other words, we can say if the vapor layer is thinner, the system will easily stabilize.

In Fig. 5, the neutral curves for the critical value of wave number with respect to the heat transfer coefficient α for the different

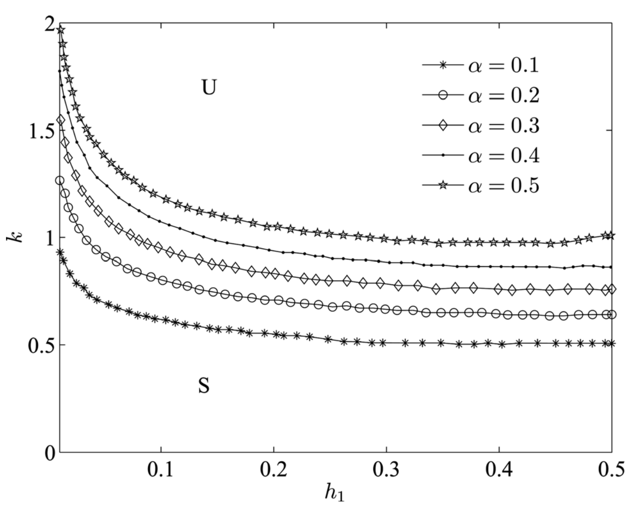

Fig. 4 The neutral curves of wave number versus vapor thickness h_1 for the different values of heat transfer coefficient α

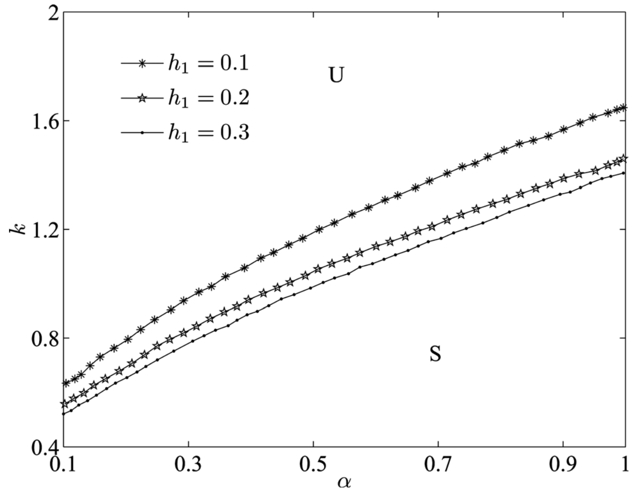

Fig. 5 The neutral curves of wave number versus heat transfer coefficient α for the different values of vapor thickness h_1

values of vapor thickness h_1 is shown. It is observed that as vapor thickness increases, the stable region decreases and so vapor thickness plays a destabilizing role. As vapor thickness increases at the crests, more evaporation will take place. This additional evaporation will increase the amplitude of the disturbance waves and the system becomes destabilized.

A comparison between the neutral curve of wave number obtained in the linear and nonlinear analysis for both inviscid and viscous potential flow analysis is made in Fig. 6 when $\alpha = 1.0\ \mathrm{gm/cm^3 s}$. It is clear from the figure that the stable region decreases in the nonlinear analysis as compared to the linear analysis for the same parametric values in inviscid as well as viscous flow analysis. This concludes that the nonlinearity reduces the stability of the system. It is also observed that viscous nonlinear analysis is more stable than inviscid nonlinear analysis, while inviscid linear analysis is more stable than nonlinear viscous analysis.

The effect of viscosity ratio of two fluids $\mu(\mu^{(1)}/\mu^{(2)})$ on the neutral curve for wave number is studied in Fig. 7. It is observed that as μ increases, the unstable region grows, which concludes that the viscosity ratio μ is destabilizing the interface. As viscosity ratio μ is directly proportional to the lower fluid viscosity and inversely proportional to the upper fluid viscosity, the lower fluid

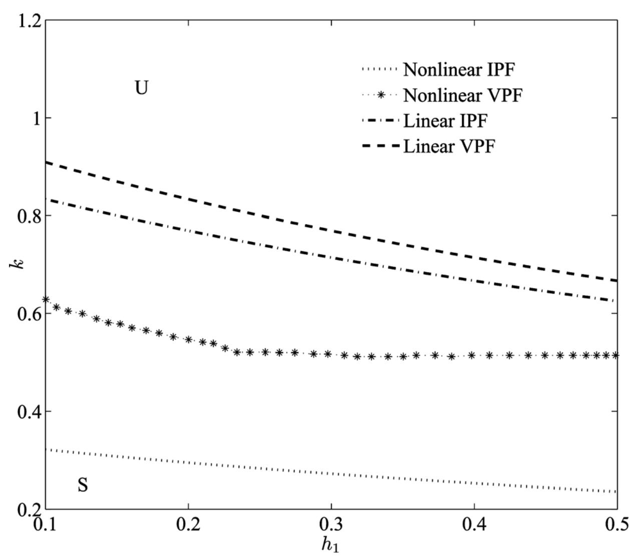

Fig. 6 Comparison between the linear and nonlinear stability analysis for vapor-water system

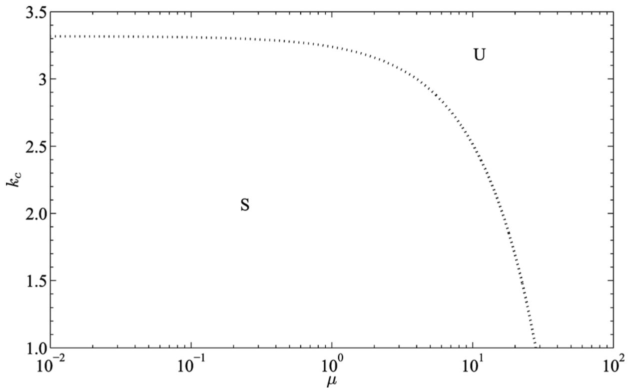

Fig. 7 The neutral curves of wave number versus viscosity ratio of two fluids $\mu(\mu^{(1)}/\mu^{(2)})$

viscosity increases the amplitudes of disturbance waves while upper phase viscosity is stabilizing the interface in the nonlinear analysis.

8 Conclusion

The nonlinear Rayleigh–Taylor instability of the interface of two viscous and incompressible fluids confined in a concentric annulus in the presence of heat and mass transfer was carried out using viscous potential flow theory. The method of multiple expansions was used for the investigation and it was shown that the evolution of the amplitude is governed by a Ginzburg–Landau equation. Nonlinearity has an important role to play on the stability of the system in the presence of heat and mass transfer. It was observed that when increasing vapor thickness, the interface is destabilizing while heat and mass transfer phenomena are stabilizing the classically unstable system. The viscosity of the upper fluid is stabilizing the interface while lower fluid viscosity destabilizes the interface. Nonlinearity reduces the region of stability.

References

[1] Hsieh, D. Y., 1972, "Effects of Heat and Mass Transfer on Rayleigh–Taylor Instability," Trans. ASME, **94**(1), pp. 156–160.
[2] Hsieh, D. Y., 1978, "Interfacial Stability With Mass and Heat Transfer," Phys. Fluids, **21**, pp. 745–748.
[3] Ho, S. P., 1980, "Linear Rayleigh-Taylor Stability of Viscous Fluids With Mass and Heat Transfer," J. Fluid Mech., **101**, pp. 111–127.
[4] Khodaparast, K. A., Kawaji, M., and Antar, B. N., 1994, "The Rayleigh–Taylor and Kelvin–Helmholtz Stability of a Viscous Liquid-Vapor Interface With Heat and Mass Transfer," Phys. Fluids, **7**, pp. 359–364.
[5] Nayak, A. R., and Chakraborty, B. B., 1984, "Kelvin–Helmholtz Stability With Mass and Heat Transfer," Phys. Fluids, **27**, pp. 1937–1941.
[6] Wu, D., and Wang, D., 1991, "The Kelvin–Helmholtz Instability of Cylindrical Flow With a Shear Layer," Mon. Not. R. Astro. Soc., **250**, pp. 760–768.
[7] Elhefnawy, A. R. F., and Radwan, A. E., 1992, "The Effect of Magnetic Fields on the Stability of a Cylindrical Flow With Mass and Heat Transfer," Phys. A, **190**, pp. 330–345.
[8] Hsieh, D. Y., 1979, "Nonlinear Rayleigh–Taylor Stability With Mass and Heat Transfer," Phys. Fluids, **22**, pp. 1435–1439.
[9] Lee, D. S., 2003, "Nonlinear Instability of Cylindrical Flow With Mass and Heat Transfer," Phys. Scr., **67**, pp. 420–426.
[10] Joseph, D. D., and Liao, T., 1994, "Potential Flows of Viscous and Viscoelastic Fluids," J. Fluid Mech., **256**, pp. 1–23.
[11] Joseph, D. D., Belanger, J., and Beavers, G. S., 1999, "Breakup of a Liquid Drop Suddenly Exposed to a High- Speed Airstream," Inter. J. Multiphase Flow, **25**, pp. 1263–1303.
[12] Joseph, D. D., Beavers, G. S., and Funada, T., 2002, "Rayleigh–Taylor Instability of Viscoelastic Drops at High Weber Numbers," J. Fluid Mech., **453**, pp. 109–132.
[13] Asthana, R., Awasthi, M. K., and Agrawal, G. S., 2012, "Viscous Potential Flow Analysis of Rayleigh–Taylor Instability of Cylindrical Interface," Appl. Mech. Mater., **110–116**, pp. 769–775.
[14] Asthana, R., and Agrawal, G. S., 2007, "Viscous Potential Flow Analysis of Kelvin–Helmholtz Instability With Mass Transfer and Vaporization," Phys. A, **382**, pp. 389–404.
[15] Awasthi, M. K., and Agrawal, G. S., 2011, "Viscous Potential Flow Analysis of Rayleigh–Taylor Instability With Heat and Mass Transfer," Int. J. Appl. Math. Mech., **7**(12), pp. 73–84. Available at http://ijamm.bc.cityu.edu.hk/ijamm/outbox/Y2011V7N12P73C9769840.pdf
[16] Kim, H. J., Kwon, S. J., Padrino, J. C., and Funada, T., 2008, "Viscous Potential Flow Analysis of Capillary Instability With Heat and Mass Transfer," J. Phys. A: Math. Theor., **41**, p. 335205.
[17] Awasthi, M. K., and Agrawal, G. S., 2012, "Nonlinear Analysis of Capillary Instability With Heat and Mass Transfer," Commun. Nonlinear Sci. Numer. Simul., **17**, pp. 2463–2475.
[18] Lange, C. G., and Newell, A. C., 1974, "A Stability Criterion for Envelope Equations," SIAM J. Appl. Math., **27**, pp. 441–456.